Cellular and Molecular Life Sciences

Research Article

Transcription factor c-Myb is involved in the regulation of the epithelial-mesenchymal transition in the avian neural crest

V. Karafiat[a†], **M. Dvorakova**[a†], **E. Krejci**[b], **J. Kralova**[a], **P. Pajer**[a], **P. Snajdr**[b], **S. Mandikova**[a], **P. Bartunek**[a], **M. Grim**[b] and **M. Dvorak**[a,*]

[a] Institute of Molecular Genetics, Academy of Sciences of the Czech Republic, 166 37 Prague (Czech Republic),
   Fax: + 420 220183586, e-mail: mdvorak@img.cas.cz
[b] Institute of Anatomy, First Faculty of Medicine, Charles University Prague, 128 00 Prague (Czech Republic)

Abstract. Multipotential neural crest cells (NCCs) originate by an epithelial-mesenchymal transition (EMT) during vertebrate embryogenesis. We show for the first time that the key hematopoietic factor c-Myb is synthesized in early chick embryos including the neural tissue and participates in the regulation of the trunk NCCs. A reduction of endogenous c-Myb protein both in tissue explants in vitro and in embryos *in ovo,* prevented the formation of migratory NCCs. A moderate over-expression of c-*myb* in naive intermediate neural plates triggered the EMT and NCC migration probably through cooperation with BMP4 signaling because (i) BMP4 activated *c-myb* expression, (ii) elevated c-Myb caused accumulation of transcripts of the BMP4 target genes *msx1* and *slug*, and (iii) the reduction of c-Myb prevented the BMP4-induced formation of NCCs. The data show that in chicken embryos, the c-*myb* gene is expressed prior to the onset of hematopoiesis and participates in the formation and migration of the trunk neural crest.

Epithelial and mesenchymal cells represent two principal cell phenotypes, which differ both in their intracellular characteristics and in their relationships to neighboring cells. While epithelial cells, owing to their cytoskeletal architecture and surface receptors for cell-to-cell interactions, form well-organized sheets of tightly connected cells, the distinct cytoskeletal organization and receptors for extracellular matrix (ECM) enable mesenchymal cells to locomote as individuals and invade their surroundings,

directed by cues from the ECM and distant cells. Epithelial and mesenchymal phenotypes are inter-convertible. This provides important means for the formation of complex body structures in metazoans because epithelial cells, upon turning into the mesenchyme, can migrate out of primitive epithelia into cell-free spaces and again adopt epithelial characteristics to give rise to new tissues. These phenotypical transformations are referred to as epithelial-mesenchymal and mesenchymal-epithelial transitions [reviewed in ref. 1]. The epithelial-mesenchymal transition (EMT) is a crucial morphogenetic event for vertebrate embryogenesis. This process is of eminent interest since it also participates in tissue repair

---

* Corresponding author.
† These authors contributed equally to this work

and regeneration and during tumor growth and metastasis [reviewed in ref. 2].

Neural crest cells (NCCs) arise in early vertebrate embryos in neural tube folds through the EMT [reviewed in refs. 3, 4]. This is a complex process programmed by a series of inductive events triggered by gradients of principal inductors, such as bone morphogenetic proteins (BMPs) and members of the Wnt family of secreted glycoproteins and fibroblast growth factor (FGF) family of growth factors [reviewed in ref. 5]. In chick embryos, BMPs appear to contribute to both early and late inductive events. Chicken BMP4 is expressed in neural folds and can transform competent cells from neural plates into migratory NCCs [6–8]. Several intracellular factors participating in neural crest development have already been recognized [reviewed in ref. 9–12]. Specifically, activation of the *slug* transcription factor and down-regulation of E-cadherin by BMP4 signaling appears to be a principal process underlying delamination of NCCs, at least in birds [13].

The *c-myb* gene is one of the key regulators of definitive hematopoiesis in vertebrates. It participates in maintaining pools of immature cells of myeloid, erythroid, and other lineages [14–16]. *c-myb* and its viral derivative transduced by AMV retrovirus were also shown to affect commitment of multipotent hematopoietic progenitors to particular blood cell lineages [17, 18]. In addition, *c-myb* appears to participate in certain developmental steps in smooth muscle cells [19], colon crypts [20], lung epithelium, hair and thyroid follicles [21], neuroretina [22], and ear [23]. *c-myb* has also long been implicated in cancer formation, including melanomas and neuroblastomas [reviewed in refs. 24–26].

E26 and AMV viral *myb* genes can transform cells of the melanocytic lineage in chicken embryo cultures [27; Karafiat et al., unpublished data]. Since melanocytes descend from the trunk neural crest, we asked whether the *c-myb* protooncogene, the parental gene of both *v-myb* oncogenes, plays any role in neural crest biology.

In this paper, we show that the c-Myb protein is likely a relevant regulator of the neural crest. We demonstrate that graded intracellular levels of the c-Myb protein are critical for the formation of migratory NCCs both in vitro and in vivo. This observation defines a novel role for the *c-myb* gene in vertebrates.

Materials and methods

Embryos, cell cultures and viruses. Brown or Barred Leghorn eggs (from the hatchery at the Institute of Molecular Genetics) were incubated until embryos reached required developmental stages. Neural fold (NF) and neural plate (NP) explants were isolated [28], collected in F12 medium supplemented with 10% horse serum, and transferred to culture dishes pre-coated with collagen type I (Sigma), 1 mg/ml. Explants were cultivated in DMEM (Sigma) with supplements [29], containing 12% fetal calf serum and 5% chick embryo extract. NPs were cultured in F12-N2 medium [30]. BMP4 (R&D Systems) was used at 300 ng/ml. Retroviral stocks were prepared from the media of virus-producing chick embryo fibroblasts (CEFs) essentially as described elsewhere [18] and concentrated tenfold on Omega 300K filters (Pall Gelman) to reach titers of 10^6/ml. The *c-myb* retrovirus arose from the pneo-ccc vector [31] rescued by MAV1 helper virus; the control myb-less construct was pneo-ccc with the c-*myb* coding sequence deleted.

Morpholino oligonucleotides. antimyb1: 5′-GTCTC-CGGGCCATCCTCGCGGCGGC, antimyb1m: 5′-GTCTgCGGcCCATC CaCGCGcCGGC (lowercase letters denote the mismatched bases) and Standard control morpholino oligonucleotidese (MO) (GeneTools) were introduced (20 μμM) into neural explants by passive transfer as described elsewhere [32]. Delivery into CEFs was achieved mainly by the scraping technique (20 μM) or by EPEI transfer (1.4 μM) [33]. Fluorescein-labeled anti-myb MO and Standard control MO were often used to monitor the oligonucleotide uptake. The cultures were analyzed after 1–6 days.

In ovo electroporation. The electroporation of chick embryos was performed as follows: 400 μM MO duplexes with DNA oligonucleotides (GeneTools, special delivery) in water and the green fluorescent protein (GFP) expression vector pCLGFPA (kindly provided by M. Scaal [34]; 10 mg/ml in phosphate-buffered saline) were mixed in the ratio 3:1. The mixture was injected into the neural tube of HH stage 10–12 embryos and electroporated using a BTX electroporator ECM 830, with the following parameters: five times 40-V square pulses of 20 ms. Efficient transfer of MOs into cells by electroporation was checked using special-delivery fluorescein-labeled MOs and pCLGFPA. Twenty-four hours after electroporation, GFP-positive embryos, identified with UV light under a dissection microscope (Olympus SZX12), were isolated and analyzed by immunohistochemistry. At least nine electroporated embryos were analyzed in each experiment.

Antibodies and immunofluorescence analysis. The rabbit polyclonal α-Myb antibody was raised against the purified full-length AMV v-Myb protein. Monoclonal antibody G3G4 (against BrdU) was from Dev. Studies Hybridoma Bank; anti-CD57 TB01 antibody against the HNK-1 epitope was generously provided by F. Malavasi. For immunofluorescence analysis, cell cultures were processed as described preveiously [18]. Prior to G3G4 antibody application, the cellular DNA was denatured in

1.5 M HCl. Images were taken with a Leica DMIRB or Olympus BX51 microscope and processed with Leica Qwin or AnalySIS (Soft Imaging System) software, respectively.

Immunohistochemistry, sections.
Embryos were fixed overnight in Serra's fluid at 4 °C, embedded in Paraplast Plus (Sherwood Medical Co.) and 8-μm sections were taken. Sections were pre-incubated with normal goat serum for 20 min at room temperature. The primary TB01 and the secondary goat anti-mouse AP (Jackson Immuno Research) antibodies were successively applied for 90 min. Immunoreactions were visualized with NBT/BCIP (Roche). Sections were then heated in a microwave in 0.1 M citrate buffer (pH 6) for 5 x 5 min, pre-incubated at 4 °C with normal rabbit and goat serum and with the monovalent goat anti-rabbit Fab fragment (Jackson), and incubated with α-Myb overnight. The secondary goat anti-rabbit HRP (Jackson) was used for 2 h at room temperature. Immunoreactions were visualized with diaminobenzidine (Sigma).

Immunohistochemistry, whole mounts. Embryos were fixed overnight in 4% paraformaldehyde/PBS/0.1% Triton, dehydrated in methanol, rehydrated, treated with proteinase K, and refixed. TB01 and secondary goat anti-mouse AP antibodies were applied overnight at 4 °C, respectively. Immunoreactions were visualized with NBT/BCIP (Roche).

Northern and western blot analyses. Total RNAs were prepared using RNAwiz (Ambion) and hybridized with c-myb or gapdh probes. Western blot analyses were performed as described preveiously [18] and developed with a Super Signal West Dura kit (Pierce). In some experiments, a densitometry and evaluation by NIH Image 1.62 software were used to compare c-Myb signal intensities.

RT-PCR. Total RNA was isolated using RNAwiz from tissue explants treated in the culture for 36 h with viruses or BMP4. Control RNAs were from untreated tissues. cDNAs were prepared using M-MLV reverse transcriptase (Promega) according to the manufacturers instructions. The cycles of semi-quantitative PCR reactions were: (95 °C 20s, 60 °C 50s, 72 °C 50s); 25 cycles with 5slug (5′-GATACCCCTCATCTTTGGGTCAGC) and 3slug (5′-GATCTGTCTGCGAAAGCCCTG) primers, 30 cycles with 5c-myb (5′-GAACAGGGACT-TCCCAGCGAAC) and 3c-myb (5′- GGTCCTCT-GAAGATGCTGCCTC) primers, 27 cycles with 5msx (5′-CACTCTGAGGAAGCACAAGACG) and 3msx (5′-GTCACTGTGCCTTTCTGATCTCC) primers, and 24 cycles with 5gapdh (5′-CCATGACAACTTTGGCATTG) and 3gapgh (5′-TCCCCACAGCCTTAGCAG) primers.

Real-time PCR. Reactions were performed (usually in triplicates) using DyNAmo SYBR Green qPCR kit (Finnzymes) on the DNA Engine Opticon2 (MJ Research) according to the manufacturer's protocol.

Results

Specificity and efficiency of polyclonal α-Myb antibody used for studies of the c-Myb role in NCCs. To investigate the c-Myb protein in neuroectoderm and NCCs, we had to develop and test the suitable α-Myb antibody. CEFs were used as test cells. The polyclonal antibody raised in rabbits against the purified, partially renatured full-length v-Myb protein from the baculovirus/insect cell expression system proved useful for c-Myb protein analyses as it specifically and reproducibly recognized different intracellular c-Myb levels in indirect immunofluorescence and on Western blots (fig. 1a, b). To achieve only a moderate over-expression of c-myb in target tissues, the recombinant c-myb retrovirus based on the MAV1 helper virus genome [31] was produced from stably transfected CEFs and concentrated by ultrafiltration. The control retroviral genome did not contain the c-myb coding sequence. With resulting retroviral stocks we were able to infect virtually every cell in the culture within 48 h, which was verified by α-gp^{MAV} antibody recognizing the MAV1 envelope glycoprotein (fig. 1c). c-Myb protein levels produced from the c-myb retrovirus were approximately two to three times higher than those of the endogenous c-Myb found in sparse fibroblasts and lower than c-Myb levels detected in primary adult bone marrow cells grown in the presence of transforming growth factors TGFα + TGFβ (T2D) and in cultured chick embryo erythroid progenitors grown in the presence of bFGF (fig. 1b).

Inhibition of c-Myb synthesis by MOs. The reduction of endogenous c-Myb protein synthesis was achieved by antisense MO antimyb1, spanning the c-myb ATG initiation codon. The control MO, antimyb1m, was the mispaired variant of antimyb1. The antimyb1 MO reduced the synthesis of endogenous c-Myb protein in sparse CEFs to approximately 20% of normal levels (fig. 1e). Another antisense MO (antimyb2) positioned 20 nucleotides upstream of antimyb1 had a weaker inhibitory effect on c-Myb synthesis. None of the other control MOs, including the standard control GeneTools oligonucleotide, displayed any observable effects (data not shown).
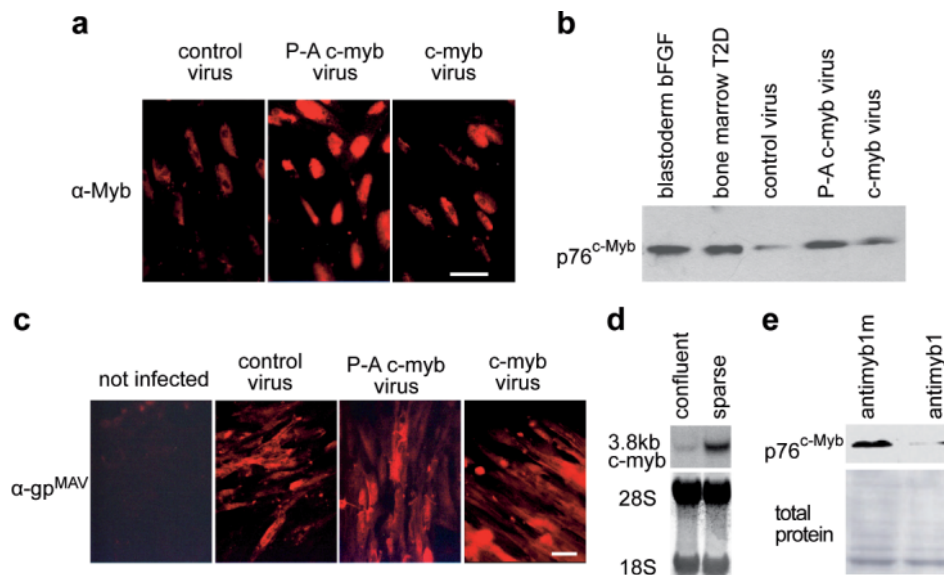
Expression of c-myb in early chick embryos. Next we analyzed c-myb expression in embryonic chick tissues at different developmental stages. Three of the early developmental stages of a chick embryo (HH stages, classifi-

cation according to Hamburger and Hamilton [35]) are schematically depicted in figure 2a. A threshold c-Myb protein synthesis was detected as early as gastrulation at chick embryo developmental stage HH 1–2, (fig. 2b, lane 6). Starting from the primitive streak stage (HH 4), both mRNA (fig. 2c, lane 1) and the protein (fig. 2b, lane 5) were relatively abundant. In HH 10–16 embryos, we found the c-Myb protein at many locations, including the neural tube (fig. 2b, lanes 1–4). Analyses of transverse sections of HH 15 embryos revealed the presence of the c-Myb protein in nuclei of the majority of cells. The highest intensity of immunoreaction with α-Myb antibody was observed in NFs, in cells delaminating from neural folds (NCs) and in dermomyotome (DM) (fig. 2d). c-Myb-positive cells delaminating from NFs were confirmed to be NCCs because they were positive for the HNK-1 epitope (fig. 2f). Figure 2f also shows the absence of c-Myb in circulating (differentiated) blood cells in aortas (LDA, RDA). No cells stained in the control experiment performed in the absence of α-Myb antibody (fig. 2e).

Certain levels of c-Myb are required for the mesenchymal phenotype. To analyze the significance of c-Myb for neural crest development, we blocked its synthesis in the HH 10 NF tissue by antimyb1 MO. This tissue (schematically depicted in fig. 3a) spontaneously generated migrating NCCs when explanted into the culture (fig. 3b). The treatment of NF explants with the control MO antimyb1m had no effect on the emigration and phenotype of NCCs (fig. 3c). However, antimyb1, which reduced the synthesis of c-Myb by approximately 50% (fig. 3j) severely blocked the formation of migratory mesenchymal cells; only a dense sheet of non-mesenchymal cells formed around explants in the presence of antimyb1 (fig. 3d). Dense sheet cells lacked typical characteristics of NCCs as they neither displayed the mesenchymal phenotype nor expressed the HNK-1 antigen, the surface marker of early migratory NCCs, unlike cells exposed to control MO (fig. 3h). Nevertheless, the 50% reduction in c-Myb did not significantly affect cell proliferation as revealed by bromodeoxyuridine (BrdU) incorporation (fig. 3i). In a typical experiment, 750 nuclei were analyzed. In antimyb1- and control oligo-treated cultures, 32.3% and 34.4% of respective nuclei were BrdU positive. This documents that a 50% reduction of c-Myb has no negative effect on the G1-S cell cycle transition but suppresses the mesenchymal phenotype. A moderate over-expression of exogenous *c-myb* (which is not inhibited by antimyb1, since its sequence upstream from ATG differs from the endogenous *c-myb*) effectively rescued the generation of mesenchymal cells from epithelia with reduced endogenous c-Myb (fig. 3e). Rescued cells contained the inhibitory oligonucleotide (verified by tracer amounts of fluorescein-labeled MO added along with antimyb MO, not shown), expressed

Figure 1. The polyclonal α-Myb antibody detects different intracellular levels of the c-Myb protein. CEFs were infected with retroviral stock prepared as described in Materials and methods. Three days later, fibroblasts were fixed and processed for immunofluorescence. (a) Detection of c-Myb in nuclei of sparse CEFs. The increment in c-Myb concentration caused by *c-myb* virus was revealed. An even higher intensity was observed after infection with the PEST domain mutant of *c-myb* (P-A *c-myb* virus). This mutation was repeatedly observed to stabilize the protein. (b) Western blot analysis of protein lysates from CEFs grown in parallel cultures as those analyzed in (a) shows the correlation between intensities of immunofluorescence and bands on Westerns. Protein lysates from chicken bone marrow cells and blastoderm cells are included for the control. Same amounts of total protein were loaded. No reaction of this antibody was observed in areas where A-Myb and B-Myb proteins would migrate. (c) Immunofluorescence analysis of the efficiency of retroviral infection. The staining of cells with the α-gp^MAV antibody against retroviral envelope antigens documents that viral stocks including those used for experiments in this paper (pneo 0 and pneo *c-myb*) contain a comparable amount of infectious particles that can infect essentially every cell in culture within 3 days. (d) Northern blot analysis documents that sparse CEFs synthesize 3.8-kb *c-myb* mRNA. (e) Western blot analysis of c-Myb protein in sparse CEFs. These cells were used for testing and selection of the most efficient anti-myb MO. Anti-myb1 MO reproducibly inhibited c-Myb to approximately 20% of an original level. This rather efficient inhibition was achieved due to EPEI-mediated MO transfer [33].

the HNK-1 epitope, a salient feature of migratory NCCs (fig. 3f, g), contained easily detectable c-Myb in nuclei, and many of them differentiated into melanocytes after several days in culture (fig. 3k), demonstrating that the exogenous *c-myb* gene indeed rescued NCCs.

In ovo electroporation of antimyb1 causes a partial inhibition of NCC formation. Antimyb1 or antimyb1m oligonucleotides were electroporated *in ovo* into the closing neural tube along with the GFP expression vector. In these experiments, heteroduplexes of MOs and partially complementary DNA oligonucleotides (see Materials and methods) were used to ensure oligonucleotide electroporation into the same side of a neural tube as the GFP vector DNA. In several experiments, 29 efficiently electroporated and normally developing embryos were obtained and analyzed for the presence of HNK-1 epitope-positive NCCs. Twelve out of 17 embryos that received antimyb1

displayed a partial reduction in HNK-1-positive cells at the anode side, while none of 12 embryos electroporated with antimyb1m displayed any side-specific changes as documented by representative experiments (fig. 4a, b). These results show that antimyb1 oligonucleotide can also inhibit formation of NCCs in vivo.

c-Myb activates the EMT in the NP and affects BMP4 signaling. The NF represents a tissue where the EMT has already been induced. The question arises whether c-Myb solely participates in the execution of the EMT activated by other factors or whether it contributes to the inductive events. To address this question we used naïve intermediate NPs [30]. This tissue (schematically depicted in fig. 5a) does not undergo the EMT in culture, unless activated by inducers such as BMP4 [6, 11]. Moderate over-expression of the retroviral *c-myb* in the NP, however, induced delamination of cells with

Figure 2. The *c-myb* gene is expressed in the early chick embryo, including neural tissues. (a) Three stages of early chick embryogenesis. Developmental stage HH 4 (18–19 h of incubation): the primitive streak (PS) has reached its maximum length (about 1.9 mm) and Hensen node (HN) is present. Developmental stage HH 9–10 (30–36 h of incubation) is characterized by eight pairs of somites (So). Neural folds (NF) at the borders of the neural plate (NP) fuse to form the neural tube (NT). The embryo is about 4 mm long. Developmental stage HH 15–16 (50–56 h of incubation); the embryo is about 8 mm long. (b) Detection of the c-Myb protein (p76^{c-Myb}) on the Western blot in embryonic (lanes 1–6) and control (lanes 7 and 8) tissues. The total protein content in samples is revealed by Ponceau S staining. (c) Northern blot detection of 3.8-kb *c-myb* and a reference (*gapdh*) mRNAs in HH 4 and HH 10–12 embryos (lanes 1 and 2) and in the chicken lymphoid cell line BK3A (lane 3). (d) Immunohistochemical visualization of the c-Myb protein (brown staining) in the transverse section of an HH 15 embryo; neural tube (NT), neural folds (NF), delaminating neural crest (NC), dermomyotome (DM) of the somite (So). (e) Control immunohistochemical reaction performed with a similar section as in (d) but in the absence of α-Myb antibody; scale bar, 100 μm. (f) HNK-1 glycotope (violet staining) in migrating NCCs. A transverse section through the dissociated somite (13th somite) of an HH 15 embryo; NT, neural tube; LDA, left dorsal aorta; RDA, right dorsal aorta with c-Myb negative differentiated blood cells; DM, dermomyotome; scale bar, 100 μm. The boxed region enlarged x 4 in the inset shows a relatively high c-Myb concentration in emigrating NCCs and colocalization of c-Myb and the HNK-1 epitope.
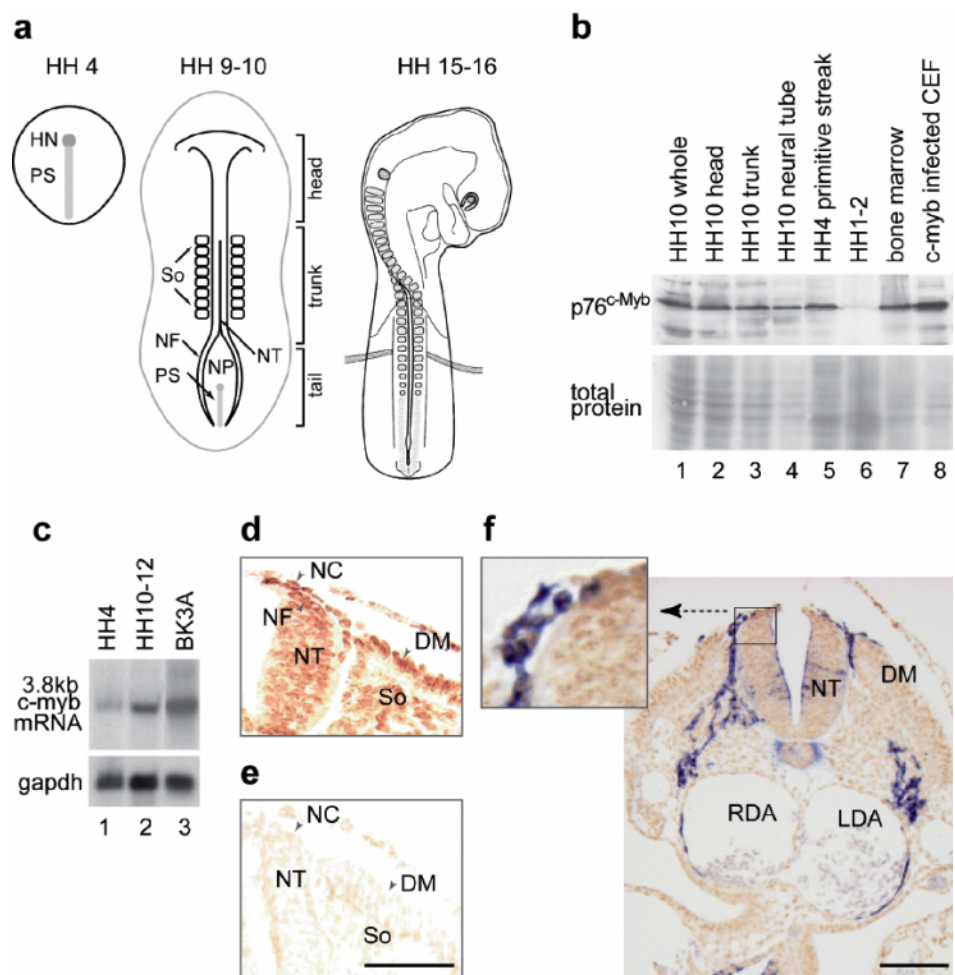
the mesenchymal phenotype, capable of differentiating into melanocytes (fig. 5b). In six independent experiments, the proportion of melanocytes was always about 25%. The analysis of NP cells by immunofluorescence revealed a relationship between c-Myb concentration and BMP4 in the activation of the EMT (fig. 5c). While control uninduced cultures contained low c-Myb and no mesenchymal HNK-1-positive NCCs (fig. 5c, first column), the BMP4 treatment induced, as expected [6, 11, 30], formation of migratory HNK-1-positive cells and also activated synthesis of endogenous c-Myb (fig. 5c, second column). Of particular interest is that antimyb1 blocked the BMP4 ability to induce mesenchymal cells

(fig. 5c, third column). In such cultures, however, the formation of migratory NCCs was efficiently rescued by the c-myb retrovirus (fig. 5c, fourth column). Thus, *c-myb* is likely one of the downstream targets of BMP4 and higher concentrations of c-Myb could activate some genes known to execute BMP4 signaling.

Elevated c-Myb causes accumulation of *msx1* and *slug* mRNAs in the NP. The semi-quantitative RT-PCR analyses revealed that higher c-Myb levels (caused by the expression of the *c-myb* virus) induced, in the naïve NP, the increase of mRNAs of *msx1* and *slug* genes (fig. 6a, NP/c-myb virus) – downstream targets of BMP4 signal-
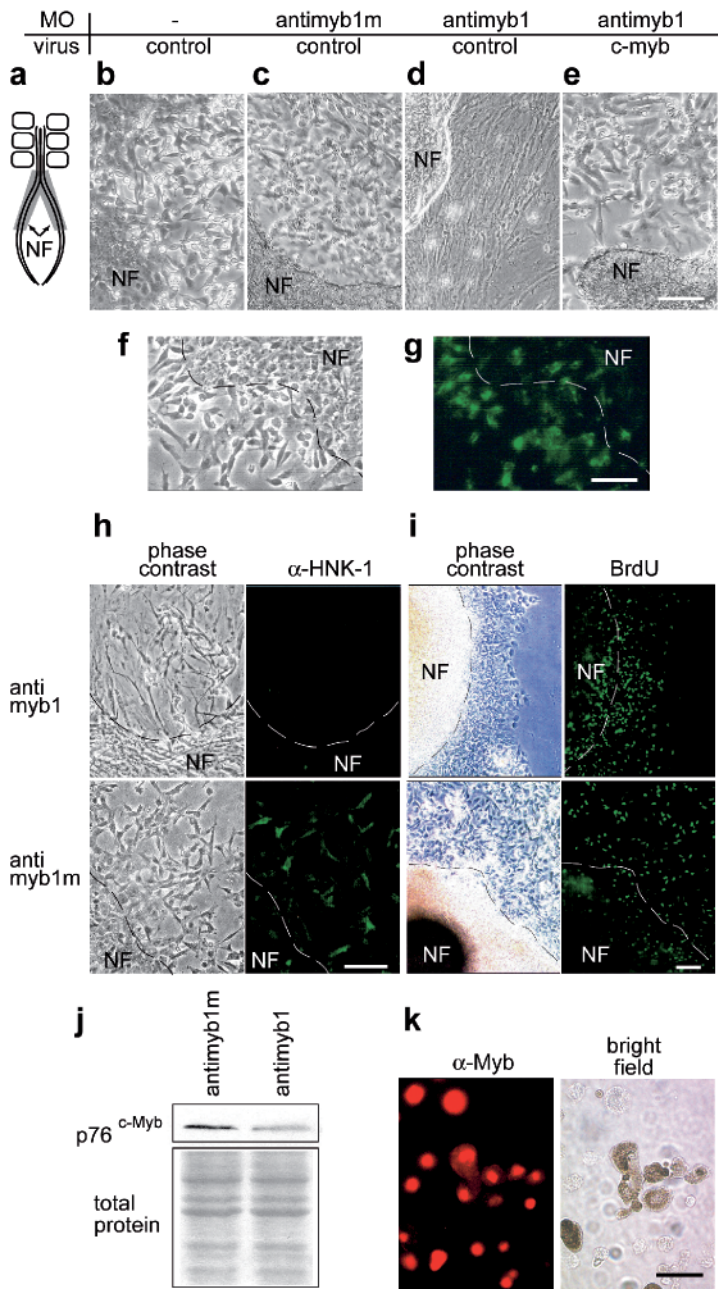

Figure 3. Formation of NCCs in the NF is c-Myb dependent. (a) The scheme of NF tissue (shaded area) in HH 10 embryos. (b–e) Phase contrast images of cells produced by NF explants under indicated conditions, after 3 days in culture. (d) The mesenchymal phenotype is inhibited by antimyb1 and rescued (e) by exogenous *c-myb*. (f, g) Mesenchymal cells rescued by exogenous *c-myb* express the HNK-1 epitope, the marker of migrating NCCs. Panels f and g represent the same field photographed in the phase contrast and under fluorescence-exciting illumination; scale bar, 100 μm. (h) The reduction of c-Myb by antimyb1 blocks formation of migrating HNK-1-positive NCCs in the explanted NF but does not significantly affect DNA synthesis measured by the incorporation of BrdU (i). (j) Upper panel: Western blot analysis of c-Myb protein concentration in NF explants exposed to MO. Lower panel: Coomasie staining of identical protein samples separated on SDS-PAGE. (k) Immunofluorescence detection of abundant c-Myb protein in nuclei of mesenchymal cells rescued in antimyb1-treated cultures by *c-myb* retrovirus; these cells differentiate into pigment cells (bright field) after 7 days; scale bar, 40 μm.
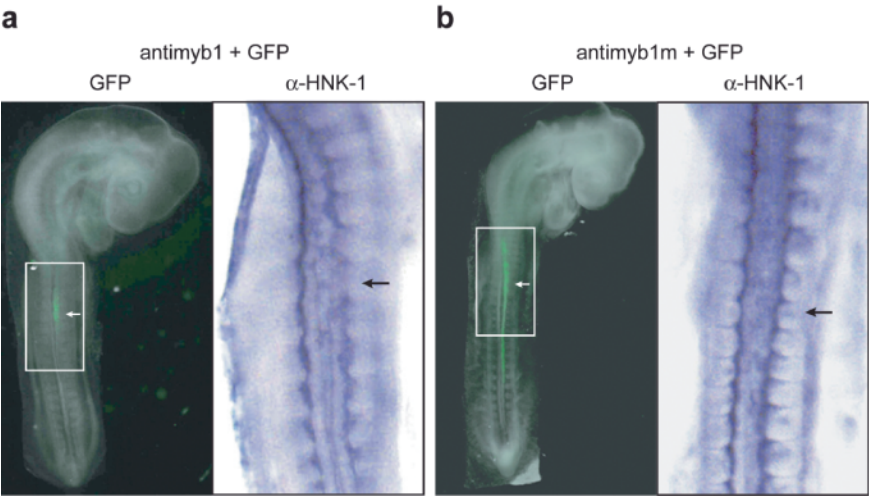
Figure 4. Antimyb1 oligonucleotide partially inhibits formation of migratory NCCs in vivo. A representative result of *in ovo* electroporations of DNA mixtures containing the GFP expression vector and the negatively charged antimyb1 morpholino heteroduplex (a) or GFP expression vector and antimyb1m control morpholino heteroduplex (b). DNA and oligonucleotides were electroporated into neural tubes of HH 12 embryos. Green fluorescence of GFP and presence of the HNK-1 epitope (violet staining) in migrating NCCs were visualized after 24 h. Arrows indicate positions of the centers of anodes. α-HNK1 panels represent higher magnification of areas delimited by white rectangles in corresponding GFP panels.

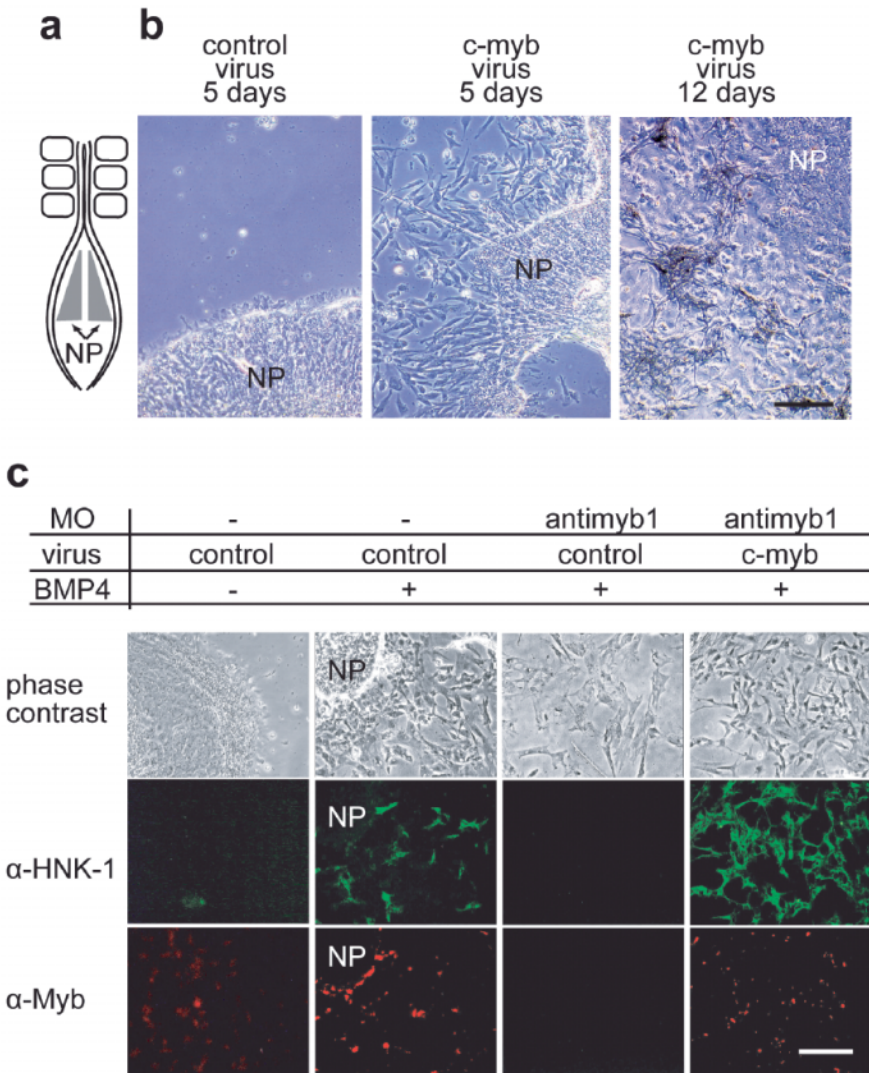Figure 5. c-Myb induces the EMT of NCCs in the NP and modulates BMP4 activity. A typical experiment (out of six similar ones) is shown. (a) Schematic drawing of the NP (shaded area) from HH 10 embryos. (b) Phase contrast images of NP explants infected with retroviruses and cultivated for the indicated time periods. Approximately 25% of the c-myb retrovirus-induced mesenchymal cells differentiate spontaneously into melanocytes (12 days in the culture). (c) BMP4 induction of the EMT is inhibited by antimyb1 and rescued by the exogenous *c-myb* transduced by the *c-myb* virus. NP explants were exposed to indicated combinations of MO, BMP4, and retroviruses, were fixed and double-labeled with α-HNK-1 and α-Myb antibodies. Each column of microphotographs shows the same field taken in the phase contrast and under fluorescence-exciting illumination. NP in the second column depicts the position of the explant. Scale bar, 80 μm.

ing [36]. The treatment of NP explants by BMP4 resulted in somewhat higher levels of these transcripts (fig. 6a, NP/BMP4), similar to levels found in NF tissue activated in a natural way within the embryo (fig. 6a, NF/not treated). BMP4 also activated the expression of endogenous *c-myb* in the NP (fig. 6a, NP/BMP4), consistent with the protein data (fig. 5c, second column). These results of semi-quantitative RT-PCR were verified in several experiments. Two independent mRNA and respective cDNA samples were prepared and repeatedly analyzed by PCR with primers specific for *msx1*, *slug*, *c-myb*, *gapdh*, and some other gene transcripts with consistent results (not shown). The levels of *slug* transcripts were also quantified by real-time PCR with identical results in three repeated experiments (fig. 6b).
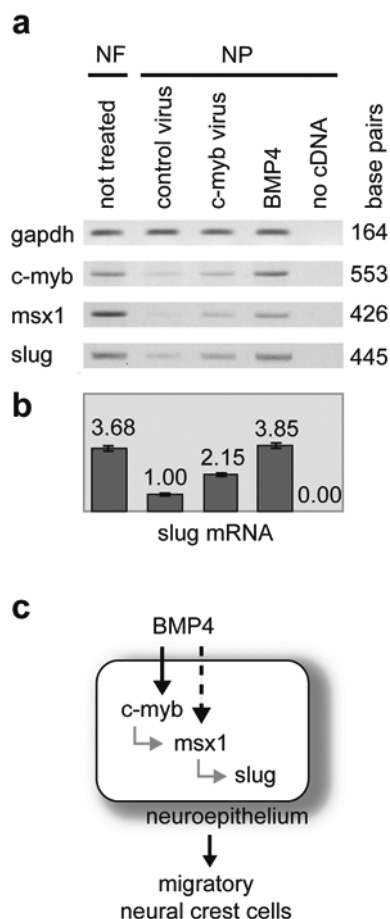
Figure 6. An elevated c-Myb concentration causes accumulation of *msx1* and *slug* gene transcripts in the NP. (a) A typical semi-quantitative RT-PCR experiment reveals levels of *gapdh*, *c-myb*, *msx1,* and *slug* mRNAs in NF and NP explants treated as indicated. (b) Determination of *slug* mRNA levels by real-time PCR in NF and treated NP tissues corresponding to samples in panel a. In the displayed experiment, triplicate reactions were run; variations are represented with error bars. (c) The proposed *c-myb* position in the BMP4-initiated cascade of gene activations during neural crest induction in NP explants. The dashed arrow represents the recently published direct activation of *msx1* transcription by the BMP4 signal [36].

Our observations suggest that c-Myb is an important mediator in the BMP4-induced formation of the neural crest, and support the notion that the BMP4-induced higher c-Myb level in neuroepithelial cells can result in the activation of *msx1* and *slug* genes whose activity causes the loss of the epithelial character and transition of competent cells into the mesenchymal state [37]. We propose that *c-myb* is an early activator of the mesenchymal phenotype in the neuroepithelium, as shown in figure 6c.

Discussion

The *c-myb* gene has been recognized as one of the key regulators of definitive hematopoiesis. In chicks, the first hematopoietic stem cells in the embryo proper appear as intra-aortic clusters at day 3 of development (HH 20) [reviewed in 38]. We found, however, that both *c-myb* mRNA and the protein were detectable at day 1 in the primitive streak stage (HH 4) and later in many cell types including the neuroectoderm and migrating NCCs. The role of c-Myb in developmental stages preceding the onset of definitive hematopoiesis in vertebrates is not well understood. Although mouse embryos with the disrupted c-*myb* gene did not display any significant abnormalities in the development of primitive hematopoietic cells [14], *c-myb* oncogenic derivatives have been demonstrated in numerous in vitro studies to regulate development of primitive avian hematopoietic cells including proliferation, differentiation, and commitment [18, 39, 40; Z. Horejsi, unpublished data]. Similarly, *c-myb*-null mice showed no phenotypes that could be caused by a defect in NC formation [14]. However, in vitro and in ovo experiments performed in this work show that c-Myb is one of the regulators of NCCs in chicks. We can speculate several explanations for these discrepancies. First, in mice, c-Myb may not be engaged in the regulation of early embryonic multipotent cells (hematopoietic and neural) while in birds and possibly other vertebrates, it is an important regulator of these cells. This view is supported by observations that *c-myb* expression is undetectable in the closing neural tube in mouse [41], but the gene is widely expressed throughout early development of frog [42] and chick embryos as documented in this work. In addition, interspecies differences in NCC patterning and subtle variations in neural tube formation [43, 44] might also reflect differences in a spectrum of genes engaged in the regulation of neural development in different early vertebrate embryos and support the view of species-specific expression/function of the *c-myb* gene. Second, *c-myb* might participate in the regulation of early developmental processes both in mice and chicks, but there might be a higher degree of genetic redundancy in mice that would eliminate the dependency of early hematopoietic and

neural cells on c-Myb functions. Currently, there are no data to confirm or disprove such speculation. Third, the lack of c-Myb function in early embryos with a disrupted or down-regulated c-Myb might be replaced by signals supporting primitive hematopoiesis and neural crest development coming from surrounding tissues or ECM and encoded by unrelated genes. Such signals would exist in intact embryos and would be largely missing in tissue cultures. In support of this third view, anti-myb morpholinos caused only a partial inhibition of NCC formation in ovo, while in tissue cultures, an essentially absolute inhibition was observed. In addition, our preliminary observations showed that at least some NCC defects caused by reduction of c-Myb in tissue culture can be complemented by specific changes in culture conditions. Further work is clearly required to shed more light on the role of c-Myb in the early development of vertebrate embryos.

Our experiments underline the significance of graded intracellular c-Myb concentrations for the biological outcome of its activity, which emerged from studies in the hematopoietic system. While zero c-Myb levels were lethal for hematopoietic progenitors [14], the low c-Myb concentration enabled survival of these cells and prompted them to develop along the macrophage and megakaryotic lineages. Higher c-Myb concentrations accentuated erythropoiesis and lymphopoiesis [17]. In this work, we observed that when 'basal' c-Myb levels in the NP are raised (approximately two- to threefold as a result of exogenous *c-myb* introduction or the BMP4 treatment), some epithelial cells undergo the EMT and give rise to NCCs. In accordance with that, immunohistochemical analyses revealed a higher intracellular concentration of c-Myb in the NF (the site of NCC emigration) and in delaminating NCCs than in the other neural tube cells. A reduction in c-Myb levels by antisense oligonucleotides in the NF (to approximatelly 50% of the initial level) blocked the EMT and formation of migratory mesenchymal cells, whose rescue was readily achieved by increased c-Myb levels. Since the formation of mesenchymal cells in atrioventricular explants was similarly dependent on c-Myb concentrations [V. Karafiat, unpublished data], we propose that in chicks, c-Myb levels are an important part of the network controlling cell-cell and/or cell-ECM interactions that participate in the formation of mesenchymal cells. Our results also suggest that c-Myb expression is enhanced by BMP4 and that c-Myb may be, at least in chicks, one of the decisive mediators of the BMP4 signal. The increased c-Myb concentration in the NP activated transcription of both *msx1* and *slug* genes. These genes have already been shown to be activated by BMP4 and are required for the formation of NCCs [6, 8, 36]. Thus, our data suggest that *c-myb* participates in the BMP4 signaling network as an activator of genes that control processes leading to loss of the epithelial character and transition of NC progenitors into the mesenchymal state. The threshold concentration of c-Myb required for the activation of the EMT during induction of NC progenitors is very likely governed by external cues including the BMP4 signaling.

The observation that c-Myb can activate the EMT suggests that the protein may be involved in initial stages of tumor metastases.

1 Hay E. D. (1995) An overview of epithelio-mesenchymal transformation. Acta Anat. **154:** 8–20

2 Thiery J. P. (2003) Epithelial-mesenchymal transitions in development and pathologies. Curr. Opin. Cell Biol. **15:** 740–746

3 Selleck M. A., and Bronner-Fraser M. (1996) The genesis of avian neural crest cells: a classic embryonic induction. Proc. Natl. Acad. Sci. USA. **93:** 9352–9357

4 Le Douarin N., and Kalcheim C. (1999) The Neural Crest. Cambridge University Press, New York

5 Aybar M. J. and Mayor R. (2002) Early induction of neural crest cells: lessons learned from frog, fish and chick. Curr. Opin. Genet. Dev**. 12:** 452–458

6 Liem K. F. Jr, Tremml G., Roelink H. and Jessell T. M. (1995) Dorsal differentiation of neural plate cells induced by BMP-mediated signals from epidermal ectoderm. Cell **82:** 969–979

7 Selleck M. A., Garcia-Castro M. I., Artinger K. B. and Bronner-Fraser M. (1998) Effects of Shh and Noggin on neural crest formation demonstrate that BMP is required in the neural tube but not ectoderm. Development **125:** 4919–4930

8 Sela-Donenfeld D. and Kalcheim C. (1999) Regulation of the onset of neural crest migration by coordinated activity of BMP4 and Noggin in the dorsal neural tube. Development **126:** 4749–4762

9 Sieber-Blum M. (2000) Factors controlling lineage specification in the neural crest. Int. Rev. Cytol. **197:** 1–33

10 Krull C. E. (2001) Segmental organization of neural crest migration. Mech. Dev. **105:** 37–45

11 Nieto M. A. (2001) The early steps of neural crest development. Mech. Dev. **105:** 27–35

12 Gammill L. S. and Bronner-Fraser M. (2003) Neural crest specification: migrating into genomics. Nat. Rev. Neurosci. **4:** 795–805

13 Cano A., Perez-Moreno M. A., Rodrigo I., Locascio A., Blanco M. J., Barrio M. G. del et al. (2000) The transcription factor snail controls epithelial-mesenchymal transitions by repressing E-cadherin expression. Nat. Cell Biol. **2:** 76–83

14 Mucenski M. L., McLain K., Kier A. B., Swerdlow S. H., Schreiner C. M., Miller T. A. et al. (1991) A functional c-myb gene is required for normal murine fetal hepatic hematopoiesis. Cell **65:** 677–689

15 Weston K. (1998) Myb proteins in life, death and differentiation. Curr. Opin. Genet. Dev. **8:** 76–81

16 Oh I. H. and Reddy E. P. (1999) The myb gene family in cell growth, differentiation and apoptosis. Oncogene **18:** 3017–3033

17 Emambokus N., Vegiopoulos A., Harman B., Jenkinson E., Anderson G., and Frampton J. (2003) Progression through key

stages of haemopoiesis is dependent on distinct threshold levels of c-Myb. EMBO J. **22:** 4478–4488

18 Karafiat V., Dvorakova M., Pajer P., Kralova J., Horejsi Z., Cermak V. et al. (2001) The leucine zipper region of Myb oncoprotein regulates the commitment of hematopoietic progenitors. Blood **98:** 3668–3676

19 Gadson P. F. Jr, Dalton, M. L., Patterson E., Svoboda D. D., Hutchinson L., Schram D. et al. (1997) Differential response of mesoderm- and neural crest-derived smooth muscle to TGF-beta1: regulation of c-myb and alpha1 (I) procollagen genes. Exp. Cell Res. **230:** 169–180

20 Zorbas M., Sicurella C., Bertoncello I., Venter D., Ellis S., Mucenski M. L. et al. (1999) c-Myb is critical for murine colon development. Oncogene **18:** 5821–5830

21 Ess K. C., Witte D. P., Bascomb C. P. and Aronow B. J. (1999) Diverse developing mouse lineages exhibit high-level c-Myb expression in immature cells and loss of expression upon differentiation. Oncogene **18:** 1103–1111

22 Plaza S., Turque N., Dozier C., Bailly M. and Saule S. (1995) C-Myb acts as transcriptional activator of the quail PAX6 (PAX-QNR) promoter through two different mechanisms. Oncogene **10:** 329–340

23 Leon Y., Miner C., Represa J. and Giraldez F. (1992) Myb p75 oncoprotein is expressed in developing otic and epibranchial placodes. Dev. Biol. **153:** 407–410

24 Thompson M. A. and Ramsay R. G. (1995) Myb: an old oncoprotein with new roles. Bioessays **17:** 341–350

25 Ganter B. and Lipsick J. S. (1999) Myb and oncogenesis. Adv. Cancer Res. **76:** 21–60

26 Ramsay R. G., Barton A. L., Gonda T. J. (2003) Targeting c-Myb expression in human disease. Expert Opin. Ther. Targets **7:** 235–248

27 Bell M. V. and Frampton J. (1999) v-Myb can transform and regulate the differentiation of melanocyte precursors. Oncogene **18:** 7226–7233

28 Selleck M. A. (1996) Culture and microsurgical manipulation of the early avian embryo. Methods Cell Biol. **51:** 1–21

29 Bartunek P., Karafiat V., Dvorakova M., Zahorova V., Mandikova S., Zenke M. et al. (1997) The Myb leucine zipper is essential for leukemogenicity of the v-Myb protein. Oncogene **15:** 2939–2949

30 Garcia-Castro M. I., Marcelle C. and Bronner-Fraser M. (2002) Ectodermal Wnt function as a neural crest inducer. Science **297:** 848–851

31 Grasser F. A., Graf T. and Lipsick J. S. (1991) Protein truncation is required for the activation of the c-myb proto-oncogene. Mol. Cell. Biol. **11:** 3987–3996

32 Kos R., Reedy M. V., Johnson R. L. and Erickson C. A. (2001) The winged-helix transcription factor FoxD3 is important for establishing the neural crest lineage and repressing melanogenesis in avian embryos. Development **128:** 1467–1479

33 Morcos P. A. (2001) Achieving efficient delivery of morpholino oligos in cultured cells. Genesis **30:** 94–102

34 Scaal M., Gros J., Lesbros C. and Marcelle C. (2004) In ovo electroporation of avian somites. Dev. Dyn. **229:** 643–650

35 Hamburger V. and Hamilton H. L. (1951) A series of normal stages in the development of the chick. J. Morphol. **88:** 49–92

36 Tribulo C., Aybar M. J., Nguyen V. H., Mullins M. C. and Mayor R. (2003) Regulation of Msx genes by a Bmp gradient is essential for neural crest specification. Development **130:** 6441–6452

37 Barrio M. G. del and Nieto M. A. (2002) Overexpression of Snail family members highlights their ability to promote chick neural crest formation. Development **129:** 1583–1593

38 Dieterlen-Lievre F. and Le Douarin N. M. (2004) From the hemangioblast to self-tolerance: a series of innovations gained from studies on the avian embryo. Mech. Dev. **121:** 1117–1128

39 Graf T. (1992) Myb: a transcriptional activator linking proliferation and differentiation in hematopoietic cells. Curr. Opin. Genet. Dev. **2:** 249–255

40 Bartunek P., Pajer P., Karafiat V., Blendinger G., Dvorak M. and Zenke M. (2002) bFGF signaling and v-Myb cooperate in sustained growth of primitive erythroid progenitors. Oncogene **21:** 400–410

41 Sitzmann J., Noben-Trauth K. and Klempnauer K. H. (1995) Expression of mouse c-myb during embryonic development. Oncogene **11:** 2273–2279

42 Amaravadi L. and King M. V. (1994) Characterization and expression of the Xenopus c-Myb homolog. Oncogene **9:** 971–974

43 Kulesa P., Ellies D. L. and Trainor P. A. (2004) Comparative analysis of neural crest cell death, migration and function during vertebrate embryogenesis. Dev. Dyn. **229:** 14–29

44 Lowery L. A. and Sive H. (2004) Strategies of vertebrate neurulation and a reevaluation of teleost neural tube formation. Mech. Dev. **121:** 1189–1197

To access this journal online:
http://www.birkhauser.ch